Proceedings of the ASME 2023
International Design Engineering Technical Conferences and Computers and Information in Engineering Conference
IDETC-CIE2023
August 20-23, 2023, Boston, Massachusetts

DETC2023-116627

HIGHER-ORDER CENTRODES AND BRESSE'S CIRCLES OF SLIDER-CRANK MECHANISMS

Chiara Lanni, Giorgio Figliolini, Luciano Tomassi

University of Cassino and Southern Lazio, Cassino, Italy

ABSTRACT

This paper deals with the formulation via the instantaneous geometric invariants of a specific algorithm to determine the higher-order centrodes and Bresse's circles for the coupler link of slider-crank mechanisms. In particular, the first, second and third order centrodes can be obtained in any configuration of the mechanism by showing the successive positions of the instant center of rotation and the acceleration and jerk poles. Several graphical and numerical results for a given slider-crank mechanism in different configuration, are also shown.

Keywords: Higher-order centrodes, higher-order Bresse's circles, instantaneous geometric invariants, slider-crank mechanisms

1. INTRODUCTION

The kinematic analysis of planar mechanisms can be usually developed through graphical and analytical methods. Among the various analytical methods there is the one that refers to the instantaneous geometric invariants, which allow to obtain simplified and compact relationships for practical applications.

The instantaneous geometric invariants were introduced by Krause in 1920 [1] and developed by Bottema [2] and Veldkamp [3]. They can be very useful in the field of kinematics from different points of view, such as the kinematic synthesis of mechanisms [4-5], the curvature analysis [6] or the design of equivalent mechanisms [7-8]. One application of the instantaneous geometric invariants is the one that refers to the centrodes, which can be utilized in various fields of machine design, as in cam mechanisms [9], cylindrical gears [10], together with kinematic synthesis of linkage [11-13]. The centrodes have been utilized also in the synthesis of spatial and spherical linkages [14-17]. The kinematic synthesis of linkage is often carried out by using some important geometric loci, as the inflection circle, the stationary circle and the cubic of stationary curvature, and the instantaneous geometric invariants can be very useful to express these geometric loci in some advantageous algebraic forms, as reported in [18]. However, geometric loci, as the ones mentioned above, along with the instant center of rotation, the acceleration and jerk centers [19-23], the Ball and Javot points, can be also of great interest for the kinematic analysis and synthesis of planar mechanisms [24-27].

The main research motivations of this paper are related to the development of the advanced planar kinematic theory for analyzing the rigid body motion with more details. In fact, increasing the order of the time-derivatives of a point position vector of a rigid body and thus, going from the velocity, to the acceleration, jerk and others, we get more instantaneously information on what the rigid body is going to do, when the previous time derivatives are equal to zero.

For example, this is the case of the incipient motions, where the velocity vectors of all points are zero, while the accelerations are different by zero. In this context, the determination of the corresponding vector fields and their poles, as the acceleration center and the jerk pole, along with the higher-order centrodes and Bresse's circles, become very useful for understanding the mechanism kinematic behavior.

In particular, this paper is devoted to the determination of the third order fixed and moving centrodes, along with the zero-normal and zero-tangential jerk circles, even to validate the right position of the jerk pole, as center of the jerk vector field of the coupler link. The proposed formulation has been obtained by using the instantaneous geometric invariants and referring to slider-crank mechanisms with constant angular velocity of the driving crank. Graphical and numerical results have allowed the validation of the proposed formulation, which has been implemented in Matlab program to obtain the first, second and third order centrodes, along with the Bresse and jerk circles, in any configuration of a given slider-crank mechanism.

2. INSTANTANEOUS GEOMETRIC INVARIANTS

Referring to the slider-crank mechanism of Fig. 1, the pairs of fixed Φ (O, X, Y) and moving f (Ω, x, y) reference frames, were chosen along with the corresponding fixed and moving canonical reference frames $\tilde{\mathcal{F}}\,(P_1, \tilde{X}, \tilde{Y})$ and $\tilde{f}\,(P_1, \tilde{x}, \tilde{y})$ which origin coincides with the instantaneous center of rotation P_1 of the coupler link AB. In particular, the $\tilde{Y}$ axis is orthogonal at P_1 point to the fixed centrode π and oriented toward the moving centrode that is not shown in Fig.1. Consequently, the $\tilde{X}$ axis is tangent to both centrodes at P_1 point and oriented clockwise with respect to the $\tilde{Y}$ axis, while the moving canonical reference frame $\tilde{f}$ is assumed as coincident with $\tilde{\mathcal{F}}$ at the referring configuration, as shown in Figure 1. The position and the orientation of the moving frame f (Ω, x, y) is obtained though the position vector $\mathbf{r}_\Omega$ which can be expressed as

$$\mathbf{r}_\Omega = r\left[\cos\delta \;\; \sin\delta\right]^T \tag{1}$$

where r and δ are the A_0A crank length and the oriented counter-clockwise angle of A_0A with respect to the X-axis, respectively. Thus, during the mechanism motion, $\mathcal{F}$ and $\tilde{\mathcal{F}}$ remain fixed to the frame, while f and $\tilde{f}$ move as attached to the coupler link AB of the slider-crank mechanism.

The instantaneous geometric invariants a_n and b_n are the n-order derivatives of the Cartesian-coordinates $\tilde{X}_I$ and $\tilde{Y}_I$ of P_1 with respect to the oriented angle ϑ that $\tilde{f}$ makes with respect to $\tilde{\mathcal{F}}$ during the coupler motion, by taking the form

$$a_n = \frac{\mathrm{d}^n \tilde{X}_I}{\mathrm{d}\vartheta^n} \quad \text{and} \quad b_n = \frac{\mathrm{d}^n \tilde{Y}_I}{\mathrm{d}\vartheta^n} \tag{2}$$

where n is a natural number.

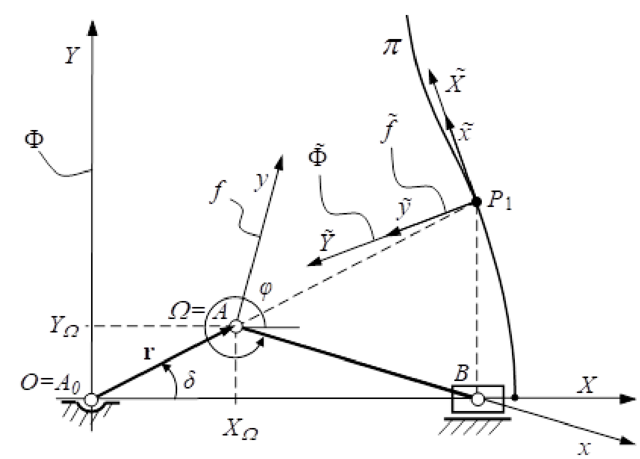

FIGURE 1: ORIGINAL(Φ AND f) AND CANONICAL ($\tilde{\mathcal{F}}$ AND $\tilde{f}$) REFERENCE FRAMES.

For a starting configuration in which both canonical frames coincide each other, as shown in Fig. 1, the instantaneous geometric invariants up to the third order are given by the following expressions:

$$a_0 = b_0 = a_1 = b_1 = a_2 = 0 \tag{3}$$

while b_2, a_3, and b_3 are different from zero and take the forms:

$$b_2 = \sqrt{\left(\frac{\mathrm{d}^2 X_\Omega}{\mathrm{d}\varphi^2} + \frac{\mathrm{d}Y_\Omega}{\mathrm{d}\varphi}\right)^2 + \left(\frac{\mathrm{d}^2 Y_\Omega}{\mathrm{d}\varphi^2} - \frac{\mathrm{d}X_\Omega}{\mathrm{d}\varphi}\right)^2} \tag{4}$$

$$\begin{aligned} a_3 = \frac{1}{b_2}\Bigg[&\left(\frac{d^3 X_\Omega}{d\varphi^3} + \frac{dX_\Omega}{d\varphi}\right)\left(\frac{d^2 Y_\Omega}{d\varphi^2} - \frac{dX_\Omega}{d\varphi}\right) + \\ &- \left(\frac{d^3 Y_\Omega}{d\varphi^3} + \frac{dY_\Omega}{d\varphi}\right)\left(\frac{d^2 X_\Omega}{d\varphi^2} + \frac{dY_\Omega}{d\varphi}\right)\Bigg] \end{aligned} \tag{5}$$

$$\begin{aligned} b_3 = \frac{1}{b_2}\Bigg[&\left(\frac{\mathrm{d}^3 X_\Omega}{\mathrm{d}\varphi^3} + \frac{\mathrm{d}X_\Omega}{\mathrm{d}\varphi}\right)\left(\frac{\mathrm{d}^2 X_\Omega}{\mathrm{d}\varphi^2} + \frac{\mathrm{d}Y_\Omega}{\mathrm{d}\varphi}\right) + \\ &+ \left(\frac{\mathrm{d}^3 Y_\Omega}{\mathrm{d}\varphi^3} + \frac{\mathrm{d}Y_\Omega}{\mathrm{d}\varphi}\right)\left(\frac{\mathrm{d}^2 Y_\Omega}{\mathrm{d}\varphi^2} - \frac{\mathrm{d}X_\Omega}{\mathrm{d}\varphi}\right)\Bigg] \end{aligned} \tag{6}$$

Referring to Eq. (1), the first, second and third derivatives with respect to the angle φ of the Cartesian coordinates X_Ω and Y_Ω that represent the components of the position vector $\mathbf{r}_\Omega$, are given by

$$\frac{\mathrm{d}X_\Omega}{\mathrm{d}\varphi} = -r\sin\delta\frac{\mathrm{d}\delta}{\mathrm{d}\varphi} \qquad \frac{\mathrm{d}Y_\Omega}{\mathrm{d}\varphi} = r\cos\delta\frac{\mathrm{d}\delta}{\mathrm{d}\varphi} \tag{7}$$

$$\begin{aligned} \frac{\mathrm{d}^2 X_\Omega}{\mathrm{d}\varphi^2} &= -r\left[\cos\delta\left(\frac{\mathrm{d}\delta}{\mathrm{d}\varphi}\right)^2 + \sin\delta\frac{\mathrm{d}^2\delta}{\mathrm{d}\varphi^2}\right] \\ \frac{\mathrm{d}^2 Y_\Omega}{\mathrm{d}\varphi^2} &= -r\left[\sin\delta\left(\frac{\mathrm{d}\delta}{\mathrm{d}\varphi}\right)^2 - \cos\delta\frac{\mathrm{d}^2\delta}{\mathrm{d}\varphi^2}\right] \end{aligned} \tag{8}$$

$$\begin{aligned} \frac{\mathrm{d}^3 X_\Omega}{\mathrm{d}\varphi^3} &= r\left[\sin\delta\left(\frac{\mathrm{d}\delta}{\mathrm{d}\varphi}\right)^3 - 3\cos\delta\frac{\mathrm{d}\delta}{\mathrm{d}\varphi}\frac{\mathrm{d}^2\delta}{\mathrm{d}\varphi^2} - \sin\delta\frac{\mathrm{d}^3\delta}{\mathrm{d}\varphi^3}\right] \\ \frac{\mathrm{d}^3 Y_\Omega}{\mathrm{d}\varphi^3} &= -r\left[\cos\delta\left(\frac{\mathrm{d}\delta}{\mathrm{d}\varphi}\right)^3 + 3\sin\delta\frac{\mathrm{d}\delta}{\mathrm{d}\varphi}\frac{\mathrm{d}^2\delta}{\mathrm{d}\varphi^2} - \cos\delta\frac{\mathrm{d}^3\delta}{\mathrm{d}\varphi^3}\right] \end{aligned} \tag{9}$$

Similarly, the first, second and third derivatives of the crank angle δ with respect to φ, can be expressed as follows:

$$\sin\delta = -\frac{l\sin\varphi}{r} \tag{10}$$

$$\frac{\mathrm{d}\delta}{\mathrm{d}\varphi} = -\frac{l\cos\varphi}{r\cos\delta} \tag{11}$$

$$\frac{\mathrm{d}^2\delta}{\mathrm{d}\varphi^2}=\frac{l\left(\sin\varphi\cos\delta-\cos\varphi\sin\delta\dfrac{\mathrm{d}\delta}{\mathrm{d}\varphi}\right)}{r\cos^2\delta} \tag{12}$$

$$\begin{aligned}\frac{\mathrm{d}^3\delta}{\mathrm{d}\varphi^3}=\frac{l}{r\cos^3\delta}\Bigg\{&\left[-\cos\varphi\left(\frac{\mathrm{d}\delta}{\mathrm{d}\varphi}\right)^2\left(\cos^2\delta-2\sin^2\delta\right)\right]+\\&+\cos\delta\sin\delta\left(2\sin\varphi\frac{\mathrm{d}\delta}{\mathrm{d}\varphi}-\cos\varphi\frac{\mathrm{d}^2\delta}{\mathrm{d}\varphi^2}\right)+\cos^2\delta\cos\varphi\Bigg\}\end{aligned} \tag{13}$$

The proposed formulation allows the computations of the instantaneous geometric invariants a_n and b_n for n = 0, 1, 2, 3, which are very useful to express in a canonical algebraic form, the most significant geometric loci with respect to $\tilde{f}\,(P_1,\tilde{x},\tilde{y})$.

This computation can be very complex when referring to the canonical frames directly, from which the convenience to make use of a different pair of frames, as f and $\mathcal{F}$, which are closer to the mechanism motion than the canonical frames.

Similarly, the first, second and third derivatives of the crank angle φ with respect to δ, can be expressed as follows:

$$\varphi=\sin^{-1}\left(-\frac{r}{l}\sin\delta\right) \tag{14}$$

$$\dot{\varphi}=\frac{d\varphi}{d\delta}=-\frac{r\cos\delta}{l\cos\varphi}\dot{\delta} \tag{15}$$

$$\ddot{\varphi}=\frac{d^2\varphi}{d\delta^2}=\frac{\dot{\delta}^2 r\sin\delta\cos\varphi-\ddot{\delta}r\cos\delta\cos\varphi}{l\cos^2\varphi}+\frac{\dot{\delta}^2r^2\cos^2\delta\sin\varphi}{l\cos^3\varphi} \tag{16}$$

$$\begin{aligned}\dddot{\varphi}=\frac{d^3\varphi}{d\delta^3}=-\frac{1}{l\cos^3\varphi}\Bigg[&r\cos^2\varphi\Big(\beta\cos\delta-3\dot{\delta}\ddot{\delta}\sin\delta+\\&-\dot{\delta}^3\cos\delta\Big)-\frac{r^3\dot{\delta}^3\cos^3\delta}{l^2}+\frac{\dot{\delta}r^2\cos\delta\sin\varphi}{l\cos\varphi}\cdot\\&\cdot\left(\dot{\delta}^2\sin\delta-\ddot{\delta}\cos\delta+\frac{r\dot{\delta}^2\cos^2\delta\sin\varphi}{l\cos^2\varphi}\right)+\\&+\frac{2\dot{\delta}r^2\cos\delta}{l}\left(\dot{\delta}^2\sin\varphi\sin\delta-\ddot{\delta}\sin\varphi\cos\delta+\frac{\dot{\delta}^2r\cos^2\delta}{l\cos^2\varphi}\right)\Bigg]\end{aligned} \tag{17}$$

3. HIGHER ORDER CENTRODES

By considering the fixed frame $\mathcal{F}$ and f as attached to the coupler link AB of the slider-crank mechanism the position of generic point M can be expressed as.

$$\begin{aligned}X_M&=r_{\Omega x}+x_M\cos\varphi-y_M\sin\varphi\\Y_M&=r_{\Omega y}+x_M\sin\varphi+y_M\cos\varphi\end{aligned} \tag{18}$$

When $M\equiv P_1$ in Eqs. (18), the parametric equations of the first order of fixed centrode λ_1 can be written as

$$\begin{aligned}X_{P1}&=r_{\Omega x}+x_{P1}\cos\varphi-y_{P1}\sin\varphi\\Y_{P1}&=r_{\Omega y}+x_{P1}\sin\varphi+y_{P1}\cos\varphi\end{aligned} \tag{19}$$

Because of P_1 is the instantaneous center of rotation $\frac{dX_{P1}}{dt}=\frac{dY_{P1}}{dt}=0$ and substituting Eqs. (7), one can obtain the parametric equations of the first order of moving centrode l_1 as

$$\begin{aligned}x_{P1}&=l\cos\varphi\left(\tan\delta\sin\varphi+\cos\varphi\right)\\y_{P1}&=l\cos\varphi\left(\tan\delta\cos\varphi-\sin\varphi\right)\end{aligned} \tag{20}$$

When $M\equiv P_2$ in Eqs. (18), the parametric equations of the second order of fixed centrode λ_2 can be written as

$$\begin{aligned}X_{P2}&=r_{\Omega x}+x_{P2}\cos\varphi-y_{P2}\sin\varphi\\Y_{P2}&=r_{\Omega y}+x_{P2}\sin\varphi+y_{P2}\cos\varphi\end{aligned} \tag{21}$$

Parametric equations of the second order of moving centrode l_2 can be obtained when $\frac{dX_{P2}}{dt}=\frac{dY_{P2}}{dt}=0$, in Eqs. (21) as

$$\begin{aligned}x_{P2}=\frac{1}{\dot{\varphi}^4+\ddot{\varphi}^2}\Bigg[&\left(\frac{\mathrm{d}^2X_\Omega}{\mathrm{d}\varphi^2}\cos\varphi+\frac{\mathrm{d}^2Y_\Omega}{\mathrm{d}\varphi^2}\cos\varphi\right)\dot{\varphi}^4+\\&+\left(\frac{\mathrm{d}X_\Omega}{\mathrm{d}\varphi}\cos\varphi+\frac{\mathrm{d}^2X_\Omega}{\mathrm{d}\varphi^2}\sin\varphi+\frac{\mathrm{d}Y_\Omega}{\mathrm{d}\varphi}\sin\varphi\right.\\&\left.-\frac{\mathrm{d}^2Y_\Omega}{\mathrm{d}\varphi^2}\cos\varphi\right)\dot{\varphi}^2\ddot{\varphi}+\left(\frac{dX_\Omega}{d\varphi}\sin\varphi+\right.\\&\left.-\frac{dY_\Omega}{d\varphi}\cos\varphi\right)\ddot{\varphi}^2\Bigg]\\y_{P2}=\frac{1}{\dot{\varphi}^4+\ddot{\varphi}^2}\Bigg[&\left(-\frac{\mathrm{d}^2X_\Omega}{\mathrm{d}\varphi^2}\cos\varphi+\frac{\mathrm{d}^2Y_\Omega}{\mathrm{d}\varphi^2}\cos\varphi\right)\dot{\varphi}^4+\\&\left(-\frac{\mathrm{d}X_\Omega}{\mathrm{d}\varphi}\sin\varphi+\frac{\mathrm{d}^2X_\Omega}{\mathrm{d}\varphi^2}\cos\varphi+\frac{\mathrm{d}Y_\Omega}{\mathrm{d}\varphi}\cos\varphi+\right.\\&\left.+\frac{\mathrm{d}^2Y_\Omega}{\mathrm{d}\varphi^2}\sin\varphi\right)\dot{\varphi}^2\ddot{\varphi}+\left(\frac{\mathrm{d}X_\Omega}{\mathrm{d}\varphi}\cos\varphi+\right.\\&\left.+\frac{\mathrm{d}Y_\Omega}{\mathrm{d}\varphi}\sin\varphi\right)\ddot{\varphi}^2\Bigg]\end{aligned} \tag{22}$$

When $M\equiv P_3$, Eqs. (18) the parametric equations of the third order of fixed centrode λ_3 can be written as

$$
\begin{aligned}
X_{P3} &= r_{\Omega x} + x_{P3}\cos\varphi - y_{P3}\sin\varphi \\
Y_{P2} &= r_{\Omega y} + x_{P2}\sin\varphi + y_{P2}\cos\varphi
\end{aligned}
\tag{23}
$$

Parametric equations of the third order of moving centrode l_3 can be obtained when $\frac{dX_{P3}}{dt} = \frac{dY_{P3}}{dt} = 0$, in Eqs. (23) as

$$
\begin{aligned}
x_{P3} = \frac{1}{\dot\varphi^6 - 2\dot\varphi^3\dddot\varphi + 9\dot\varphi^2\ddot\varphi^2 + \dddot\varphi^2}\Bigg[&\left(-\frac{\mathrm{d}^3X_\Omega}{\mathrm{d}\varphi^3}\sin\varphi + \frac{\mathrm{d}^3Y_\Omega}{\mathrm{d}\varphi^3}\cos\varphi\right)\dot\varphi^6 + \\
&+3\left(-\frac{\mathrm{d}^2X_\Omega}{\mathrm{d}\varphi^2}\sin\varphi + \frac{\mathrm{d}^2Y_\Omega}{\mathrm{d}\varphi^2}\cos\varphi + \frac{\mathrm{d}^3X_\Omega}{\mathrm{d}\varphi^3}\cos\varphi + \frac{\mathrm{d}^3Y_\Omega}{\mathrm{d}\varphi^3}\sin\varphi\right)\dot\varphi_1^4\ddot\varphi + \\
&+\left(-\frac{\mathrm{d}X_\Omega}{\mathrm{d}\varphi}\sin\varphi + \frac{\mathrm{d}Y_\Omega}{\mathrm{d}\varphi}\cos\varphi + \frac{\mathrm{d}^3X_\Omega}{\mathrm{d}\varphi^3}\sin\varphi - \frac{\mathrm{d}^3Y_\Omega}{\mathrm{d}\varphi^3}\cos\varphi\right)\dot\varphi^3\dddot\varphi + \\
&+9\left(\frac{\mathrm{d}^2X_\Omega}{\mathrm{d}\varphi^2}\cos\varphi + \frac{\mathrm{d}^2Y_\Omega}{\mathrm{d}\varphi^2}\sin\varphi\right)\dot\varphi^2\ddot\varphi^2 + \\
&+3\left(\frac{\mathrm{d}X_\Omega}{\mathrm{d}\varphi}\cos\varphi + \frac{\mathrm{d}Y_\Omega}{\mathrm{d}\varphi}\sin\varphi + \frac{\mathrm{d}^2X_\Omega}{\mathrm{d}\varphi^2}\sin\varphi - \frac{\mathrm{d}^2Y_\Omega}{\mathrm{d}\varphi^2}\cos\varphi\right)\dot\varphi\ddot\varphi\dddot\varphi + \\
&+\left(\frac{\mathrm{d}X_\Omega}{\mathrm{d}\varphi}\sin\varphi + \frac{\mathrm{d}Y_\Omega}{\mathrm{d}\varphi}\cos\varphi\right)\dddot\varphi^2\Bigg]
\end{aligned}
\tag{24}
$$

$$
\begin{aligned}
y_{P3} = \frac{1}{\dot\varphi^6 - 2\dot\varphi^3\dddot\varphi + 9\dot\varphi^2\ddot\varphi^2 + \dddot\varphi^2}\Bigg[&\left(-\frac{\mathrm{d}^3X_\Omega}{\mathrm{d}\varphi^3}\cos\varphi - \frac{\mathrm{d}^3Y_\Omega}{\mathrm{d}\varphi^3}\sin\varphi\right)\dot\varphi^6 + \\
&+3\left(\frac{\mathrm{d}^2X_\Omega}{\mathrm{d}\varphi^2}\cos\varphi - \frac{\mathrm{d}^2Y_\Omega}{\mathrm{d}\varphi^2}\sin\varphi - \frac{\mathrm{d}^3X_\Omega}{\mathrm{d}\varphi^3}\sin\varphi + \frac{\mathrm{d}^3Y_\Omega}{\mathrm{d}\varphi^3}\cos\varphi\right)\dot\varphi^4\ddot\varphi + \\
&+\left(-\frac{\mathrm{d}X_\Omega}{\mathrm{d}\varphi}\cos\varphi - \frac{\mathrm{d}Y_\Omega}{\mathrm{d}\varphi}\sin\varphi + \frac{\mathrm{d}^3X_\Omega}{\mathrm{d}\varphi^3}\cos\varphi + \frac{\mathrm{d}^3Y_\Omega}{\mathrm{d}\varphi^3}\sin\varphi\right)\dot\varphi^3\dddot\varphi + \\
&+9\left(-\frac{\mathrm{d}^2X_\Omega}{\mathrm{d}\varphi^2}\sin\varphi + \frac{\mathrm{d}^2Y_\Omega}{\mathrm{d}\varphi^2}\cos\varphi\right)\dot\varphi^2\ddot\varphi^2 + \\
&+3\left(\frac{\mathrm{d}X_\Omega}{\mathrm{d}\varphi}\sin\varphi + \frac{\mathrm{d}Y_\Omega}{\mathrm{d}\varphi}\cos\varphi + \frac{\mathrm{d}^2X_\Omega}{\mathrm{d}\varphi^2}\cos\varphi + \frac{\mathrm{d}^2Y_\Omega}{\mathrm{d}\varphi^2}\sin\varphi\right)\dot\varphi\ddot\varphi\dddot\varphi + \\
&+\left(\frac{\mathrm{d}X_\Omega}{\mathrm{d}\varphi}\cos\varphi + \frac{\mathrm{d}Y_\Omega}{\mathrm{d}\varphi}\sin\varphi\right)\dddot\varphi^2\Bigg]
\end{aligned}
$$

4. BRESSE AND JERK CIRCLES

The geometric loci of kinematic interest are the Bresse's and jerk circles. They can be expressed in an algebraic form by referring to the moving via the instantaneous geometric invariants. In particular, referring to the moving canonical reference frame $\tilde f\,(P_1, \tilde x, \tilde y)$, one has the following algebraic equation for the inflection circle $\mathcal{I}$:

$$
\tilde x^2 + \tilde y^2 - b_2\,\tilde y = 0 \tag{25}
$$

where b_2 is obtained by the Eq. (4).

The stationary circle $\mathcal{S}$ or second Bresse's circle takes the form:

$$
\ddot\varphi\left(\tilde x^2 + \tilde y^2\right) + b_2\,\dot\varphi^2\,\tilde x = 0 \tag{26}
$$

where $\dot\varphi$ and $\ddot\varphi$ represent the angular velocity and acceleration, respectively. Thus, the acceleration center P_2 can be obtained as intersection of the two Bresse's circles.

The zero-normal jerk circle $\mathcal{J_N}$ has the following algebraic equation:

$$
3\,\ddot\varphi\left(\tilde x^2 + \tilde y^2\right) - a_3\,\dot\varphi^2\,\tilde x - \left(b_3\,\dot\varphi^2 + 3b_2\,\ddot\varphi\right)\tilde y = 0 \tag{27}
$$

where a_3 and b_3 are obtained by Eqs. (5) and (6), while $\dot\varphi$ and $\ddot\varphi$ are the angular velocity and acceleration in Eqs. (15) and (16).

The zero-tangential jerk circle $\mathcal{J_T}$ has the following algebraic equation:

$$
\left(\dddot\varphi - \dot\varphi^3\right)\left(\tilde x^2 + \tilde y^2\right) + \left(b_3\,\dot\varphi^3 + 3b_2\,\ddot\varphi\,\dot\varphi\right)\tilde x - a_3\,\dot\varphi^3\,\tilde y = 0 \tag{28}
$$

where b_2, a_3 and b_3 are obtained as reported above, while $\dddot\varphi$ is the angular jerk in Eq. (17).

Consequently, the jerk pole P_3 can be obtained by intersecting the zero-normal and zero-tangential jerk circles, where the first intersection is still located at P_1, as shown in Fig. 2. Excluding the inflection circle of Eq. (25), the geometric loci given by the algebraic Eqs. (26), (27) and (28) take into account the kinematic properties of the coupler motion of the planar mechanism, that is they depend on the angular velocity $\dot\varphi$, the angular acceleration $\ddot\varphi$ and the angular jerk $\dddot\varphi$, respectively, and not only by the geometric properties given by the instantaneous invariants b_2, a_3 and b_3. Instead, the inflection circle, since representing the geometric locus of all coupler points showing an inflection point in their trajectory, only depends on b_2.

5. GRAPHICAL AND NUMERICAL RESULTS

The proposed formulation has been implemented in Matlab for validation purposes and significant graphical and numerical results have been obtained for different sizes and configurations of the slider-crank mechanism.

In particular, Figs. 2 and 3 show the 2nd order fixed λ_2 and moving l_2 centrodes, along with the Bresse circles, which intersect each other at the acceleration pole P_2 for the crank angles $\varphi = 60°$ and 0°, respectively.

Similarly, Figs. 4 and 5 show the 3rd order fixed λ_3 and moving l_3 centrodes, along with the jerk circles, which intersect at the jerk pole P_3 for the crank angles φ = 60° and 0°, respectively.

Finally, Figs. 6 and 7 show all together the 1st, 2nd and 3rd order fixed and moving centrodes for the crank angles $\varphi = 60°$ and 0°, respectively, along with P_1, P_2 and P_3.

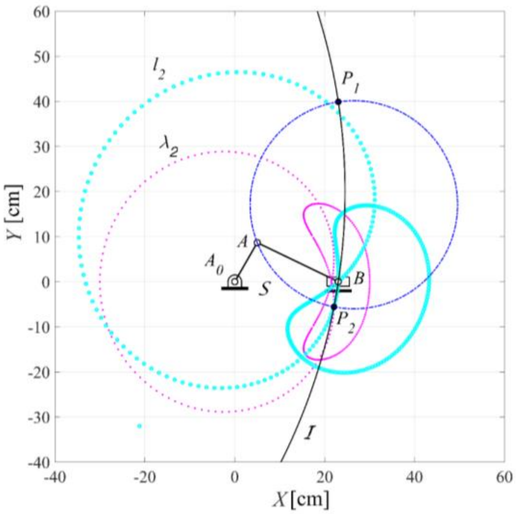

FIGURE 2: 2ND ORDER CENTRODES AND BRESSE'S CIRCLES FOR $\varphi = 60°$.

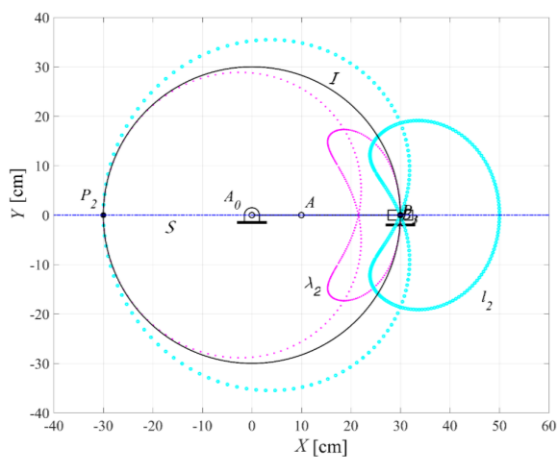

FIGURE 3: 2ND ORDER CENTRODES AND BRESSE'S CIRCLES FOR $\varphi = 0°$.

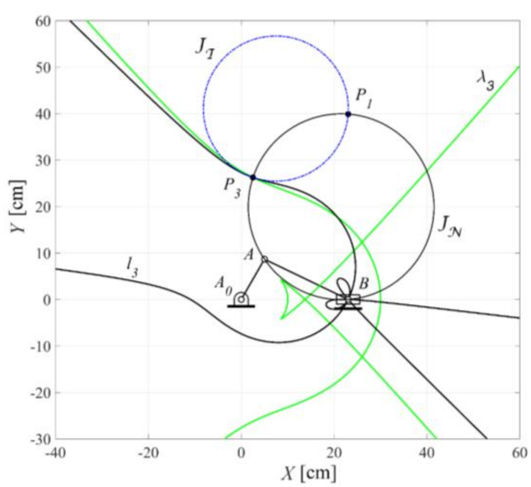

FIGURE 4: 3RD ORDER CENTRODES AND JERK CIRCLES FOR $\varphi = 60°$.

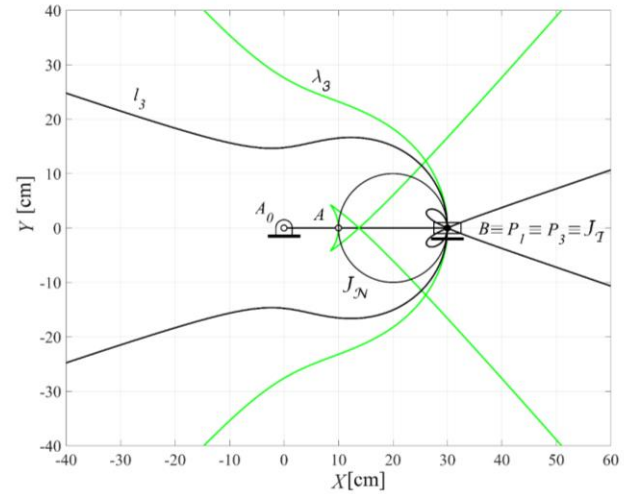

FIGURE 5: 3RD ORDER CENTRODES AND JERK CIRCLES FOR $\varphi = 0°$.

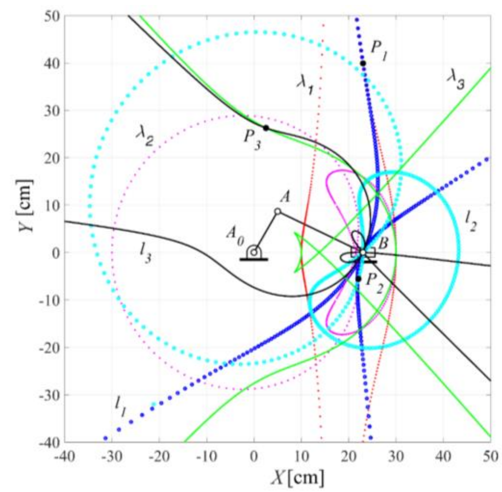

FIGURE 6: 1ST, 2ND AND 3RD ORDER FIXED AND MOVING CENTRODES FOR $\varphi = 60°$.

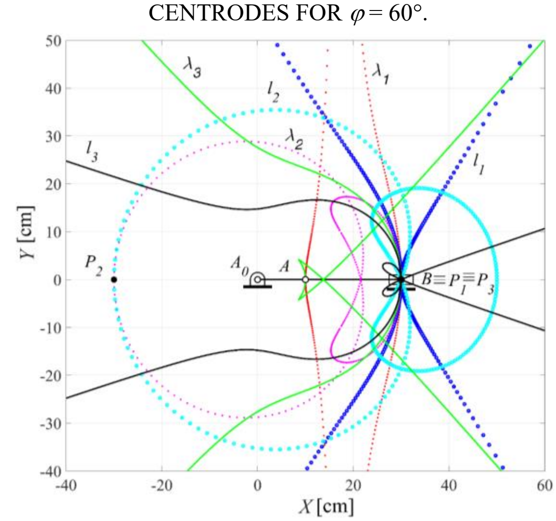

FIGURE 7: 1ST, 2ND AND 3RD ORDER FIXED AND MOVING CENTRODES FOR $\varphi = 0°$.

6. CONCLUSIONS

In order to give a contribution to the development of the advanced planar kinematic theory, a suitable formulation via the instantaneous geometric invariants of a specific algorithm to determine the higher-order centrodes and Bresse's circles for the coupler link of slider-crank mechanisms, has been proposed.

The first, second and third order centrodes can be obtained in any configuration of a given mechanism by showing the successive positions of the instant center of rotation and the acceleration and jerk poles.

Moreover, the proposed algorithm allows the animation of the mechanism, along with the first, second and third order moving centrodes, which are attached to the moving plane of the coupler link. Bresse's circles and zero–normal and zero–tangential jerk circles are also obtained with their intersection at the instant center of rotation and acceleration and jerk poles. The first order centrodes are characterized by a pure-rolling motion and geometric properties, while the second and third order centrodes are related to kinematic properties and the respective moving and fixed centrodes, intersect each other in more than one point, and one of them is the acceleration or jerk pole, respectively.

REFERENCES

[1] Krause, M. (1920). *Analysis der Ebenen Bewegung*. Berlin: Vereinigung Wissenschaftlicher Verleger, Walter De Gruyter & Co.

[2] Bottema, O. (1961). On instantaneous invariants. Proceedings of the International Conference for Teachers of Mechanisms, New Haven, CT: Yale University, pp. 159-164.

[3] Veldkamp, G.R. (1963). *Curvature theory in plane kinematics*. Groningen: J.B. Wolters.

[4] Roth, B. and Yang, A.T. (1977). Application of instantaneous invariants to the analysis and synthesis of mechanisms. *J. of Engineering for Industry*, 99(1), pp. 97–103.

[5] Bottema, O. and Roth, B. (1990). *Theoretical kinematics*. New York: Dover.

[6] Yang, A.T., Pennock, G.R. and Hsia, L.-M. (1994). Instantaneous invariants and curvature analysis of a planar four-link mechanism. *J. of Mechanical Design*, 116(4), pp. 1173–1176.

[7] Di Benedetto, A. and Pennestrì E. (1991). *Introduzione alla cinematica dei meccanismi*. Milano: Casa Editrice Ambrosiana.

[8] Roth, B. (2015). On the advantages of instantaneous invariants and geometric kinematics. *Mechanism and Machine Theory*, 89, pp. 5–13.

[9] Figliolini G., Rea P., Angeles J. (2006). The pure-rolling cam-equivalent of the Geneva mechanism. *Mechanism and Machine Theory*, 41 (11), pp. 1320–1335.

[10] Figliolini, G., Lanni, C., Sorli, M. (2022). Kinematic Analysis and Centrodes Between Rotating Tool with Reciprocating Motion and Workpiece. In: Niola V., Gasparetto A., Quaglia G., Carbone G. (Eds.): IFToMM Italy 2022, Mechanisms and Machine Science, 2022, 122 MMS, pp. 54–60.

[11] Figliolini G., Stachel H., Angeles J. (2015). Base curves of involute cylindrical gears via Aronhold's first theorem. *Proceedings of the Institution of Mechanical Engineers, Part C: Journal of Mechanical Engineering Science*, 230 (7-8), pp. 1233– 242.

[12] Figliolini G., Lanni C. (2019). Jerk and jounce relevance for the kinematic performance of long-dwell mechanisms. 15th IFToMM World Congress, Krakow, Poland, paper n.0079, 2019.

[13] Tomassi, L., Lanni, C., Figliolini, G. (2022). A Novel Design Method of Four-Bar Linkages Mimicking the Human Knee Joint in the Sagittal Plane. In: Niola, V., Gasparetto, A., Quaglia, G., Carbone, G. (eds) Advances in Italian Mechanism Science. IFToMM Italy 2022. Mechanisms and Machine Science, vol 122. Springer, Cham

[14] Kamphuis, H.J. (1969). Application of spherical instantaneous kinematics to the spherical slider-crank mechanism. *Journal of Mechanisms*, 4(1), pp. 43–56.

[15] Figliolini, G. and Angeles, J. (2017). The spherical equivalent of Bresse's circles: The case of Crossed Double-crank linkages. *Journal of Mechanisms and Robotics*, 9(1).

[16] Figliolini G., Lanni C., Kaur R. (2019). Kinematic Synthesis of Spherical Four-bar Linkages for Five-Poses Rigid Body Guidance. Uhl T. (eds) Advances in Mechanism and Machine Science. IFToMM WC 2019. Mechanisms and Machine Science, vol 73. Springer, Cham, pp.639-648

[17] Inalcik, A., Ersoy, S. and Stachel, H. (2015). On instantaneous invariants of hyperbolic planes. *Mathematics and Mechanics of Solids*, 22(5), pp. 1047–1057.

[18] Figliolini, G., Conte, M. and Rea, P. (2012). Algebraic algorithm for the kinematic analysis of slider-crank/rocker mechanisms. *Journal of Mechanisms and Robotics*, 4(1).

[19] Rees, E.L. (1923). Vectorial treatment of the motion of a rigid body in a plane. *The American Mathematical Monthly*, 30 (6), pp. 290–296.

[20] Schiller, R.W. (1965). Method for determining the instantaneous center of acceleration for a given link. *Journal of Applied Mechanics*, 32 (1), pp. 217–218

[21] Sun, H. and Liu, T. (2009). Analysis of instantaneous center of zero acceleration of rigid body in planar motion. *Modern Applied Science*, 3 (4), pp. 191–195.

[22] Carter, W.J. (1958). Second acceleration in four-bar mechanisms as related to Rotopole motion. *Journal of Applied Mechanics*, 25 (2), pp. 293–294.

[23] Chiang, C.H. (1972). Graphical angular jerk analysis of four-bar linkages. *Mech. and Machine Theory*, 7 (4), pp. 407–419.

[24] Hwang, W.M. and Fan, Y.S. (2008) "Polynomial equations for the loci of the acceleration pole of a slider-crank mechanism," *Mechanism and Machine Theory*, 43 (2), pp. 123–137.

[25] Figliolini G., Lanni C. (2018). Geometric loci for the kinematic analysis of planar mechanisms via the instantaneous geometric invariants, MEDER: Proc. of the 4th IFT0MM Symposium on Mechanism Design, Gasparetto A. & Ceccarelli M. (Eds.), Springer, Cham, 184-192.

[26] Figliolini G., Lanni C., Tomassi L. (2020). Kinematic Analysis of Slider – Crank Mechanisms via the Bresse and Jerk's Circles. Carcaterra A., Paolone A., Graziani G. (eds) Proc. of XXIV AIMETA 2019. Lecture Notes in Mechanical Engineering. Springer, Cham. pp.278-284.

[27] Figliolini G., Lanni C., Tomassi L. (2022). First and Second Order Centrodes of Slider-Crank Mechanisms by Using Instantaneous Invariants. Altuzarra O., Kecskeméthy A. (eds.) Springer Proc. in Advanced Robotics. ARK 2022. 18th Int. Symposium on Advances in Robot Kinematics, 24 SPAR, Springer, pp. 303 – 310.